Thermal population of the $4f^15d^1$ state in $BaSO_4:Pr^{3+}$

A. P. Vink, P. Dorenbos, and C. W. E. van Eijk
Interfaculty Reactor Institute, Delft University of Technology, Mekelweg 15, 2629 JB Delft, The Netherlands
(Received 14 February 2002; revised manuscript received 30 May 2002; published 26 August 2002)

Temperature-dependent measurements of luminescent intensity and lifetimes of the $4f^2[^1S_0 \rightarrow {}^1I_6]$ and $4f^15d^1 \rightarrow 4f^2$ emission for $BaSO_4:Pr^{3+}$ were performed. It was found that the intensity of the $4f^15d^1$ emission, relative to the $4f^2$ emission, increases with higher temperature, and that the decay time of the $^1S_0 \rightarrow {}^1I_6$ emission decreases from 190 to 56 ns. From both intensity and decay-time measurements an energy barrier between the $4f^2[^1S_0]$ level and the first $4f^15d^1$ state of about 0.04 eV was found. At $T=10$ K also $4f^15d^1 \rightarrow 4f^2$ emission can be observed, which has a decay time of 10 ns. Emission from the $4f^15d^1$ state at low temperature is not thermally coupled with emission from the $^1S_0$ state, but originates directly (not via the $^1S_0$ level) from excitation in the $4f^15d^1$ band. This emission can be excited efficiently when pumping on the low-energy side of the $4f^15d^1$ excitation band. This phenomenon of direct $4f^15d^1 \rightarrow 4f^2$ emission is only visible at low temperature as at higher temperatures, it is obscured by the $4f^15d^1$ emission originating from the thermal population of the $4f^15d^1$ state from the $^1S_0$ level.

DOI: 10.1103/PhysRevB.66.075118 PACS number(s): 78.55.Hx, 71.70.Ch

I. INTRODUCTION

The lanthanide ion Pr^{3+} has the [Xe] $4f^2$ configuration. The energy-level scheme is shown in Fig. 1. All the $4f^2$ energy levels are below 25 000 cm^{-1} except for the $^1S_0$ level, which is located at about 47 000 cm^{-1}. In Fig. 1, a two-step emission process, where $^1S_0 \rightarrow {}^1I_6$ emission is followed by $^3P_0 \rightarrow {}^3H_4$ emission, is shown. This is known as quantum cutting or photon cascade emission. The quantum cutting process, i.e., gaining two emitted photons from one absorbed photon, is interesting for phosphors applied in lighting or plasma display panels. Quantum cutting was discovered in 1974 for $YF_3:Pr^{3+}$[1,2] and has been reported for several fluoride,[1–5] aluminate,[6,7] borate[8,9] and sulfate[10–12] hosts.

To obtain quantum cutting, the lowest-energy levels of the $4f^15d^1$ configuration must be above the relatively isolated $^1S_0$ level. Otherwise, excitation in the $4f^15d^1$ states leads to parity-allowed emission from the lowest $4f^15d^1$ state to different $4f^2$ levels. Using Pr^{3+} in these hosts is not interesting for the applications mentioned above, but could instead be interesting for application in fast scintillator materials.

In this paper, the thermal population of the lowest $4f^15d^1$ state is studied for $BaSO_4:Pr^{3+}$. The vacuum ultraviolet and visible spectroscopy of $BaSO_4:Pr^{3+}$ and other Pr^{3+}-doped sulfates was described earlier by van der Kolk *et al.*[11] Both $4f^15d^1 \rightarrow 4f^2$ and $4f^2[^1S_0 \rightarrow {}^{2S+1}L_J]$ emissions were observed. At first, it was suggested that there was emission from two different Pr^{3+} sites. The results also revealed that at low temperatures the $4f^2[^1S_0 \rightarrow {}^{2S+1}L_J]$ emissions dominated, whereas at higher temperatures the $4f^15d^1 \rightarrow 4f^2$ emission became stronger in intensity. The behavior of these two different types of emission will be studied by measuring both the intensity and lifetime at the different temperatures. From this data it is possible to determine the energy barrier ΔE between the $^1S_0$ level and the first $4f^15d^1$ state.

To determine ΔE, a three-level scheme can be assumed and the equation used for Cr^{3+} in emerald and ruby by Kisliuk and Moore[13] can then be rewritten for the case of Pr^{3+},

$$\tau^{-1} = A_{\text{tot}} = \frac{A_f + A_d \exp(-\Delta E/kT)}{1 + \exp(-\Delta E/kT)}, \tag{1}$$

where A_{tot} is the total transition probability of the $4f^2[^1S_0]$ state, A_f is the transition probability of the $4f^2[^1S_0 \rightarrow {}^{2S+1}L_J]$ transitions and A_d is the transition probability of the $4f^15d^1 \rightarrow 4f^2$ transitions, k is Boltzmann's constant, and T is the temperature. In the limit $T \rightarrow 0$, $A_{\text{tot}} = A_f$, whereas for $T \rightarrow \infty$ $A_{\text{tot}} = (A_f + A_d)/2$.

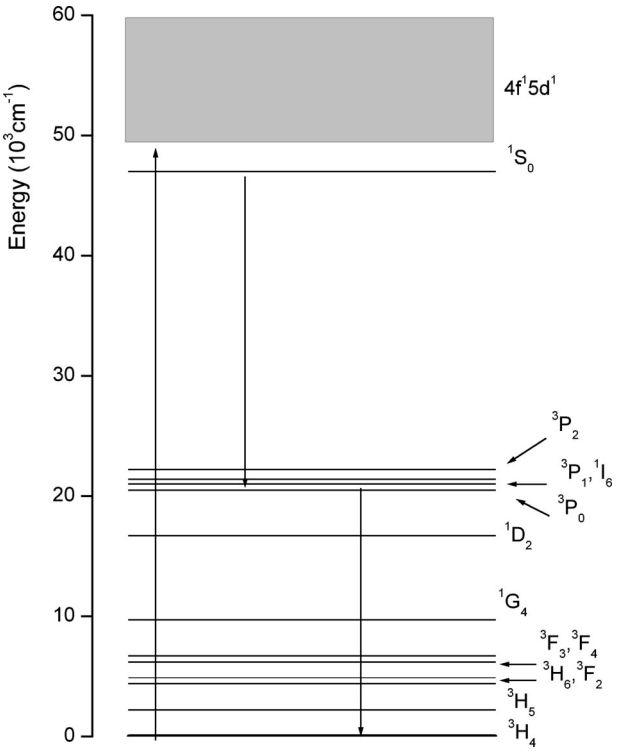

FIG. 1. Energy-level scheme of Pr^{3+} showing, after excitation in the $4f^15d^1$ state, two-step emission ($^1S_0 \rightarrow {}^1I_6$ and $^3P_0 \rightarrow {}^3H_4$) to the ground state.

As the intensity I scales with the radiative transition probability A, a similar expression as Eq. (1) can be written for the temperature dependence of the intensity of the $4f^2[^1S_0 \rightarrow ^{2S+1}L_J]$ and the $4f^15d^1 \rightarrow 4f^2$ emission lines. It is also possible to express the intensity ratio R as[14]

$$R = \frac{I_f}{I_d} = C \exp\left(\frac{\Delta E}{kT}\right), \tag{2}$$

where R is the intensity ratio between all $4f^15d^1 \rightarrow 4f^2$ (I_d) and $4f^2[^1S_0 \rightarrow ^{2S+1}L_J]$ (I_f) and C is a constant.

The physics on thermal population and determination of the energy barrier ΔE from intensity and lifetime measurements are not new. Here this effect is observed for the $4f^2$ and $4f^15d^1$ states of Pr^{3+}. Besides for the transition-metal ion Cr^{3+}, thermal population was also observed for the divalent lanthanides Eu^{2+} $(4f^7)$ (Refs. 14–16) and Sm^{2+} $(4f^6)$,[18] where the opposite-parity $4f^{n-1}5d^1$ state is at much lower energy than in the corresponding isoelectronic trivalent lanthanides (Gd^{3+} and Eu^{3+}, respectively).

In literature, ΔE values are known for different Eu^{2+}-doped compounds. For Eu^{2+} in fluorides, energy values such as 1290 cm^{-1} ($LiBaF_3$),[17] 1000 cm^{-1} ($SrAlF_5$),[15] and 970 cm^{-1} ($RbMgF_3$) were reported.[16] Meijerink measured the energy barrier by probing both the temperature dependence of decay time and intensity and found two different values: 1290 cm^{-1} from lifetime measurements and 600 cm^{-1} from intensity measurements.[17] The energy value is much lower for $SrB_4O_7:Eu^{2+}$ (130 cm^{-1}),[19] whereas for the fluorohalides values ranging from 702 cm^{-1} (SrFCl) to 202 cm^{-1} ($BaFCl_{0.5}Br_{0.5}$) are known.[20] A study of Eu^{2+}-doped beryllium silicates yielded values of 0.15 eV (1210 cm^{-1}) for $SrBe_2Si_2O_7$ and 0.09 eV (726 cm^{-1}) for $BaBe_2Si_2O_7$.[14] For Sm^{2+}-doped SrF_2, a ΔE value of 533 cm^{-1} was reported.[16]

The effect of thermal population was also found for $BaSO_4:Eu^{2+}$, but no analysis of the intensity at different temperatures was performed.[21] More recently Shen and Bray described thermal population for Sm^{2+} in MFCl (M: Ba, Sr, Ca) crystals. Population of the $4f^65d^1$ did not result in $4f^55d^1 \rightarrow 4f^7$ emission, but in nonradiative relaxation to the $^5D_2$ and $^5D_1$ levels at elevated temperatures.[18] However, to our knowledge no thermal analysis has been made on any Pr^{3+}-doped host.

II. EXPERIMENTAL

Pr^{3+}-doped $BaSO_4$ was synthesized using usual solid state techniques. $Pr_2(SO_4)_3$ was stoichiometricly mixed with $BaSO_4$ and fired in a tube oven at approximately 950 °C for 8 h under air. The Pr^{3+} concentration was 0.5 mole %. The purity of the sample was checked using x-ray diffraction and the sample proved to be of single phase.

The temperature dependent and time-resolved measurements for $BaSO_4:Pr^{3+}$ were performed on the Deutsches Electronen Synchotron (DESY) using the SUPERLUMI setup at HASYLAB. Details on the excitation setup can be found somewhere else.[22] The spectral region in excitation is 50-300 nm with a resolution of 0.3 nm. The luminescence was detected using a water-cooled photomultiplier tube (200–600 nm region) with a spectral resolution in emission of about 1 nm. Time-resolved experiments were performed using a Canberra multichannel analyzer. The time between bunches was 200 ns. Besides time-averaged excitation spectra, excitation spectra using two different time windows with a delay time τ_d and a gate time τ_g were measured. For the first time window, denoted as the fast spectrum $\tau_d = 0$ ns and $\tau_g = 13$ ns. and for the second time window, denoted as the slow spectrum $\tau_d = 80$ ns and $\tau_g = 81$ ns.

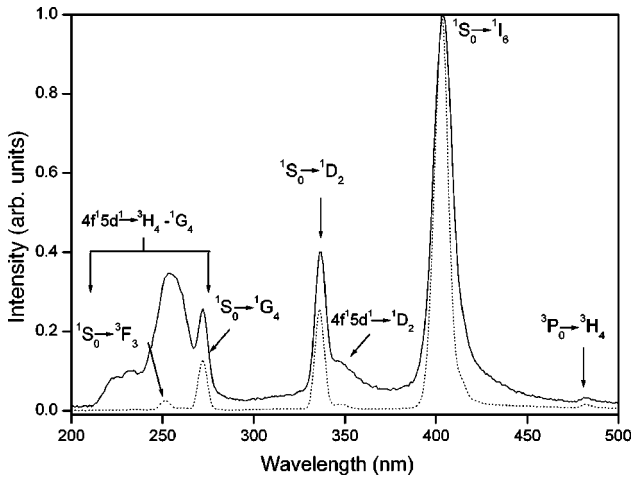

FIG. 2. Emission spectra ($\lambda_{exc} = 188$ nm) of $BaSO_4:Pr^{3+}$ at $T = 10$ K (dashed line) and 292 K (solid line).

III. RESULTS AND DISCUSSION

In Fig. 2, emission spectra ($\lambda_{exc} = 188$ nm) of $BaSO_4:Pr^{3+}$ at 10 K and 292 K are shown. The spectra are normalized at the $^1S_0 \rightarrow ^1I_6$ transition. Besides $4f^2 \rightarrow 4f^2$ transitions from the $^1S_0$ level, $4f^15d^1$ transitions to different $4f^2$ levels are visible. The relative intensity of the $4f^15d^1$ transitions is much higher at room temperature than at $T = 10$ K. This provides a first indication that thermal occupation of the lowest energy $4f^15d^1$ band from the $^1S_0$ $(4f^2)$ level occurs. The intensity ratio of the $4f^2$ and $4f^15d^1$ emissions can be fit to Eq. (2) thus determining ΔE. It is not necessary to determine the intensities of all the $4f^15d^1 \rightarrow 4f^2$ (I_d) and $4f^2[^1S_0 \rightarrow ^{2S+1}L_J]$ (I_f) transitions. We have chosen to determine the intensity of only the $^1S_0 \rightarrow ^1I_6$ and of the $4f^15d^1$ emissions in the spectral region between 220 and 290 nm. In this region not only $4f^15d^1 \rightarrow 4f^2$ emission, but also $4f^2$ $[^1S_0 \rightarrow ^1G_4, ^3F_3]$ emission can be observed. A correction for this contribution was made. The intensity ratio R between the $4f^15d^1$ and $^1S_0 \rightarrow ^1I_6$ transition as $\ln(R)$ for two excitation wavelengths ($\lambda_{exc} = 188$ nm and $\lambda_{exc} = 205$ nm) as a function of $1/T$ is shown in Fig. 3. A linear fit to Eq. (2) gives a $\Delta E = 0.041$ eV, corresponding to 325 cm^{-1}.

Extrapolating the curve shown in Fig. 3 to $T = 10$ K predicts that the $4f^15d^1$ state is not populated via the $^1S_0$ level at this temperature. However, $4f^15d^1 \rightarrow 4f^2$ emission can be observed. In Fig. 4, time-resolved emission spectra, measured at $T = 10$ K and in the wavelength region of 225–425

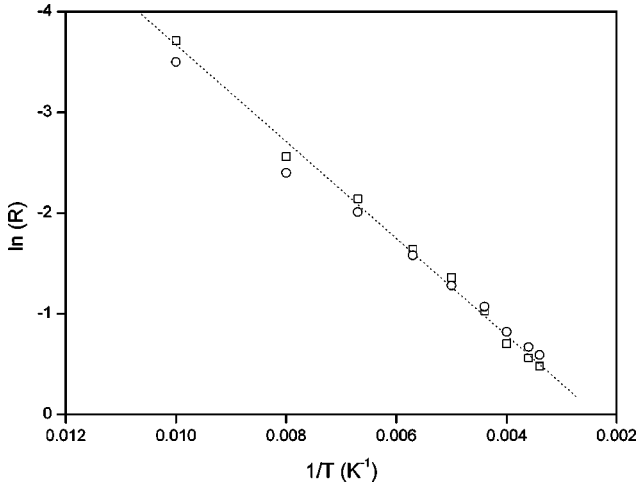

FIG. 3. Arrhenius plot showing the intensity ratio (ln R) between the $4f^15d^1 \rightarrow {}^3H_4$ and ${}^1S_0 \rightarrow {}^1I_6$ emission at different temperatures ($1/T$). The data points are shown using two different excitation wavelengths (rectangle:$\lambda_{exc}=188$ nm, circle:$\lambda_{exc}=205$ nm). A least-squares fit to Eq. (2) is shown.

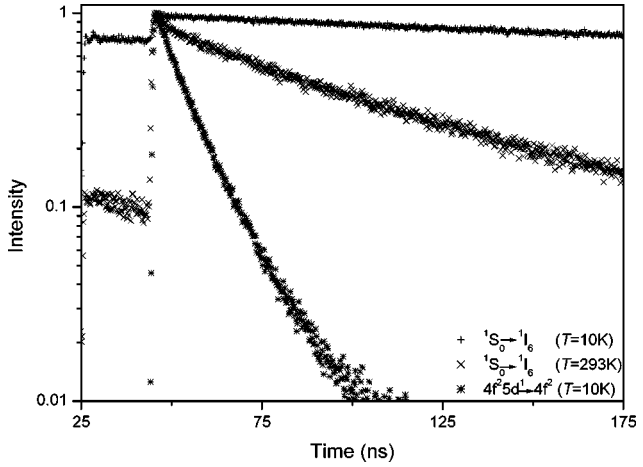

FIG. 5. Decay curve of $BaSO_4:Pr^{3+}$ ($\lambda_{exc}=188$ nm) of the ${}^1S_0 \rightarrow {}^1I_6$ emission ($\lambda_{em}=404$ nm) measured at $T=10$ K (+) and $T=292$ K (x) and of the $4f^15d^1$ emission ($\lambda_{em}=260$ nm) measured at $T=10$ K (*). The curves have different background intensities.

nm, are shown. In the fast spectrum, $4f^15d^1 \rightarrow 4f^2$ emission is visible. Obviously, there must be another process that contributes to $4f^15d^1 \rightarrow 4f^2$ emission at low temperatures. This process does not influence the data on the thermal population, as the intensity of the $4f^15d^1 \rightarrow 4f^2$ emission is still very small.

The decay curve of this $4f^15d^1$ emission was measured to determine if this emission is not due to thermal population. In Fig. 5 decay curves at 10 K and 293 K of both emissions are shown. The decay curves for the $4f^2[{}^1S_0 \rightarrow {}^1I_6]$ transition ($\lambda_{exc}=188$ nm, $\lambda_{em}=404$ nm) are shown at both temperatures, whereas the decay curve of the $4f^15d^1 \rightarrow 4f^2$ transitions ($\lambda_{exc}=188$ nm, $\lambda_{em}=260$ nm) is shown only at $T=10$ K. The decay time and the shape of the curve for the $4f^15d^1$ emission at $T=293$ K is the same as the curve of the $4f^2[{}^1S_0 \rightarrow {}^1I_6]$ emission. This is expected as the two states are in thermal equilibrium. The decay time of the $4f^15d^1 \rightarrow 4f^2$ emission measured at $T=10$ K is 10 ns, which is significantly smaller than the decay time of the $4f^2$ $[{}^1S_0 \rightarrow {}^{2S+1}L_J]$ emissions. This decay time is comparable with the decay time of $4f^15d^1$ emissions in materials that do not show the PCE effect, such as Pr^{3+}-doped $YAlO_3$,[23] KY_3F_{10},[24] $LiYF_4$[25] and several other fluorides.[25]

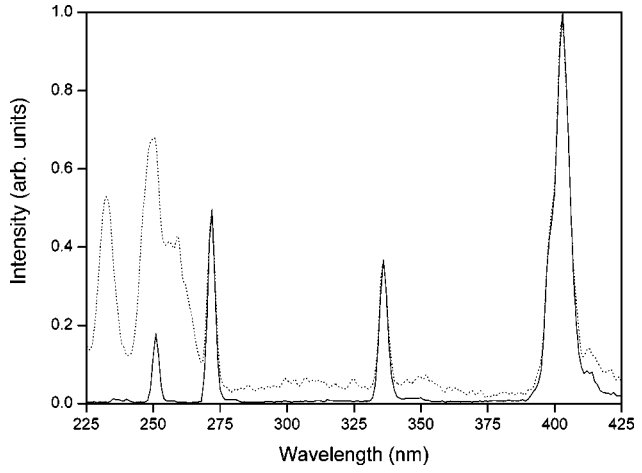

FIG. 4. Emission spectra ($\lambda_{exc}=188$ nm) of $BaSO_4:Pr^{3+}$ at $T=10$ K measured in the fast (dashed line) and slow (solid line) time region. Both spectra are normalized to the ${}^1S_0 \rightarrow {}^1I_6$ emission at 404 nm.

The decay time of the ${}^1S_0 \rightarrow {}^1I_6$ transition measured at different temperatures is shown in Table I. It decreases from 190 ± 25 ns at $T=10$ K to 56 ± 1 ns at $T=293$ K. In Fig. 6 the decay time $1/\tau$ as a function of T is shown. The values for the parameters A_f, A_d, and ΔE can be obtained from a least-squares fit to Eq. (1). ΔE was estimated to 0.040 ± 0.006 eV, corresponding to 323 ± 48 cm^{-1}, whereas $A_f = 6.24 \times 10^6$ s^{-1} and $A_d = 62.24 \times 10^6$ s^{-1}. The value of 16 ns for $1/A_d$ is in reasonable agreement with the value of 10 ns measured for the uncoupled $4f^15d^1 \rightarrow 4f^2$ emission measured at $T=10$ K.

Essentially, the value for the energy barrier ΔE deter-

TABLE I. Decay time τ of the ${}^1S_0 \rightarrow {}^1I_6$ transition at different temperatures.

Temperature (K)	Decay time τ (ns)
10	190 ± 25
50	166 ± 31
100	128 ± 20
125	114 ± 11
150	114 ± 10
175	94 ± 7
204	82 ± 3
225	83 ± 4
250	68 ± 2
273	63 ± 2
292	56 ± 1

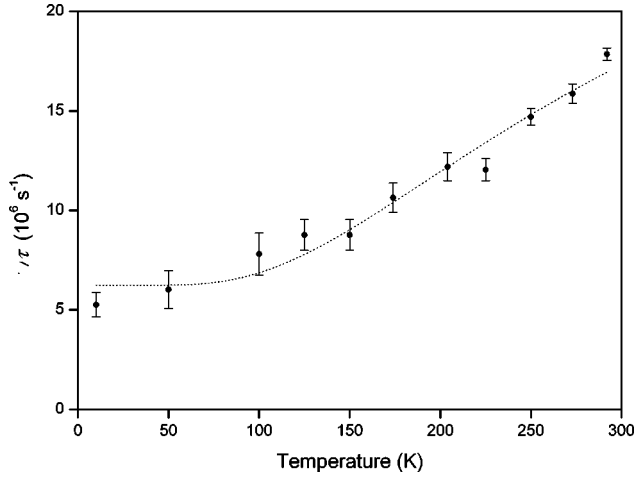

FIG. 6. Decay time $(1/\tau)$ as a function of (T) for the ${}^1S_0 \rightarrow {}^1I_6$ transition of $BaSO_4:Pr^{3+}$. A least-squares fit to Eq. (1) is shown.

mined from both decay time and intensity measurements should be comparable, which is indeed the case. An assumption in the determination of the value for ΔE from decay-time measurements is that A_f and A_d are independent of temperature. It is, however, not excluded that temperature dependence exists for the A_f and A_d parameters.

From the value for ΔE in $BaSO_4:Pr^{3+}$ and the already known data for Ce^{3+} and Pr^{3+} in $BaSO_4$, a configuration coordinate model can be constructed as is shown in Fig. 7. The energies of the $4f^2$ levels are well established. The energy difference in excitation between the ${}^1S_0$ $4f^2$ level and the first $4f^15d^1$ band is approximately 3400 cm^{-1}. A Stokes shift of about 4700 cm^{-1} could be estimated from $BaSO_4:Ce^{3+}$.[26]

The value for the decay time for the ${}^1S_0 \rightarrow {}^1I_6$ transition of $BaSO_4:Pr^{3+}$ is remarkably small (190 ns) for a $4f^2 \rightarrow 4f^2$ transition. The decay time is 850 ns for $YF_3:Pr^{3+}$ (Ref. 27) and 650 ns for $SrAl_{12}O_{19}:Pr^{3+}$.[28] The short decay time for the ${}^1S_0 \rightarrow {}^1I_6$ transition is attributed to the admixture

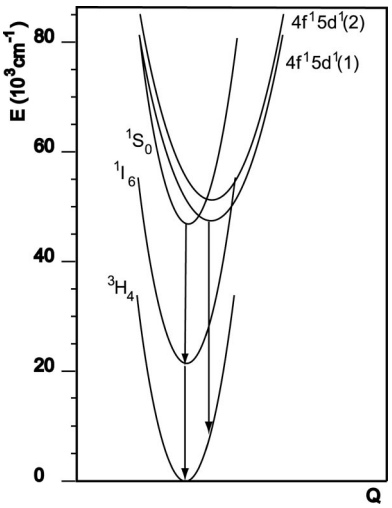

FIG. 7. The configuration coordinate diagram for $BaSO_4:Pr^{3+}$ showing the ${}^3H_4$, ${}^1I_6$, and ${}^1S_0$ $4f^2$ levels and the two lowest-energy $4f^15d^1$ bands. The vibronic levels are not shown.

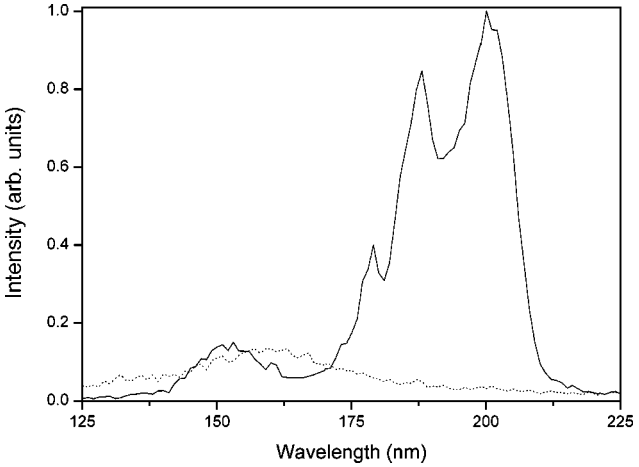

FIG. 8. Excitation spectra ($\lambda_{em}=260$ nm) of $BaSO_4:Pr^{3+}$ ($T=10$ K) measured with the fast (solid) and the slow (dashed line) time window.

of $4f^15d^1$ wave functions in the $4f^2$ ${}^1S_0$ state. Huang *et al.* has analyzed the admixture in $SrAl_{12}O_{19}:Pr^{3+}$ and has identified the $4f^15d^1$ components that mix into the ${}^1S_0$ state for this host.[28]

We now turn to the discussion of the fast emission present at $T=10$ K. This emission can be identified as $4f^15d^1$ emission that is not caused by thermal population from the $4f^2$ ${}^1S_0$ level. Time-resolved excitation spectra measured at $T=10$ K probing this emission ($\lambda_{em}=260$ nm) are shown in Fig. 8. In the fast spectrum, $4f^15d^1$ bands are clearly visible. The slow spectrum shows the SO_4^{2-} host excitation band between 140 and 160 nm.[29,30] The excitation spectrum of $4f^15d^1$ emission was also presented in Ref. 11 and differs from the excitation spectrum of the ${}^1S_0 \rightarrow {}^1I_6$ ($\lambda_{em}=404$ nm). This difference is observed in Fig. 9, where the time-averaged spectra measured at $T=10$ K, probing ${}^1S_0 \rightarrow {}^1I_6$ and the $4f^15d^1$ emission. At room temperature, the excitation spectra of both different emissions are the same, as

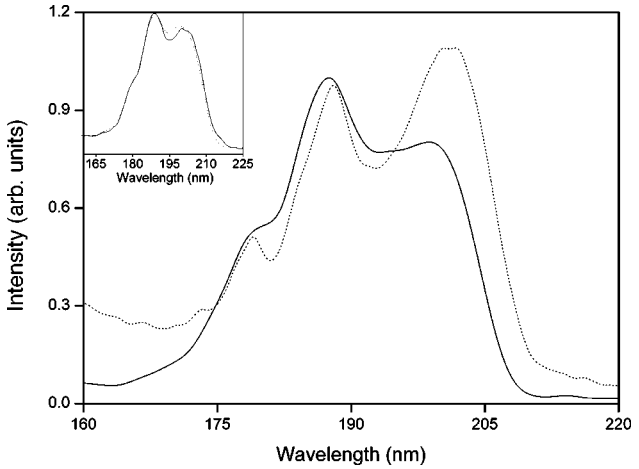

FIG. 9. Time-averaged excitation spectra of $BaSO_4$ at $T=10$ K monitoring both the $4f^15d^1 \rightarrow {}^3H_4$ ($\lambda_{em}=260$ nm, dashed line) and the ${}^1S_0 \rightarrow {}^1I_6$ ($\lambda_{em}=404$ nm, solid line) emission. The inset shows the same excitation spectra, measured at $T=292$ K.

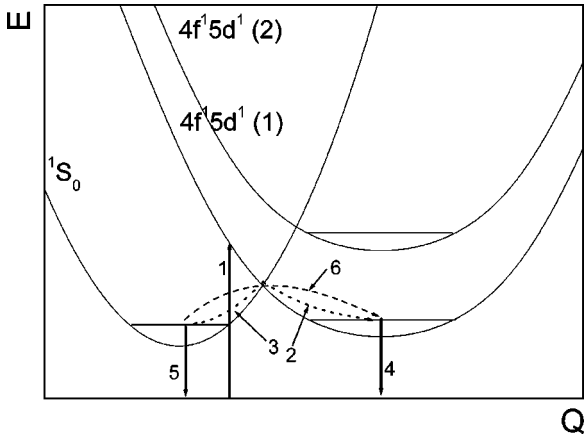

FIG. 10. The configuration coordinate diagram in the energy region of the $^1S_0$ level and $4f^15d^1$ state. Arrows 1–6 show different excitation and emission processes, which are explained in the text.

is shown in the inset of Fig. 9.

An explanation of these results can be given using the configurational coordinate diagram shown in Fig. 10. This diagram shows the energy region of the $^1S_0$ level and the first two $4f^15d^1$ states and is a magnification of Fig. 7. Different excitation and emission processes discussed below are shown in Fig. 10 as numbered arrows. At 10 K, when there is no thermal population of the $4f^15d^1$ state from the $^1S_0$ state, both the $4f^15d^1$ and the $^1S_0$ emission can be fed (arrow 2 and 3) through the excitation in the $4f^15d^1$ bands (arrow 1). Although the intensity of the $4f^15d^1$ emission (arrow 4) is almost two orders of magnitude smaller than of the $^1S_0$ (arrow 5) emission, the intensity ratio in the spectral region from 170 to 195 nm is constant (see Fig. 9). In the spectral region from 195 to 215 nm, more $4f^15d^1$ emission (compared to $^1S_0$ emission) is excited. Apparently, the probability to relax to the bottom of the $4f^15d^1$ state parabola is dependent on the excitation energy. The energy of the 205-nm absorption (48 780 cm^{-1}) is close to the energy of the intersection of the $4f^15d^1$ state with the $^1S_0$ level. Apparently, at this point, a larger number of electrons can reach the lowest-energy $4f^15d^1$ state without thermal population from the $^1S_0$ level. The excitation spectra measured at $T=292$ K (inset Fig. 9) are the same, because almost all the $4f^15d^1$ emission originates indirectly from the $^1S_0$ state (arrow 6 in Fig. 10).

IV. CONCLUSIONS

We have measured the temperature and lifetime behavior of the $4f^15d^1 \rightarrow 4f^2$ and $4f^2$ $[^1S_0 \rightarrow ^{2S+1}L_J]$ related emissions in $BaSO_4:Pr^{3+}$. The occurrence of the two different emissions was explained by assuming that, at elevated temperatures, the $4f^15d^1$ state becomes populated via the $^1S_0$ $4f^2$ level and then emits in the UV region. The energy of the barrier between the $^1S_0$ level and the $4f^15d^1$ band was determined by both temperature-dependent intensity and lifetime measurements. Possibly, this behavior is not only present in $BaSO_4:Pr^{3+}$, but also in other Pr^{3+}-doped hosts. At $T=10$ K, also $4f^15d^1$ emission is present, which originates directly from $^3H_4 \rightarrow 4f^15d^1$ excitation. The decay time of this emission is 10 ns. At higher temperatures most of the $4f^15d^1$ emission originates from the thermal population of the $^1S_0$ level and therefore the decay time is the same as for the $^1S_0 \rightarrow ^1I_6$ emission.

ACKNOWLEDGMENTS

The authors thank Mrs. R.C. Perego for the synthesis of the $BaSO_4:Pr^{3+}$ sample and Dr. M. Kirm (HASYLAB, DESY Hamburg) for his assistance for the experiments performed on the SUPERLUMI setup. These investigations were supported by the Dutch Technology Foundation (STW) and by the IHP Contract No. HPRI-CT-1999-00040 of the European Commission.

[1] W.W. Piper, J.A. deLuca, and F.S. Ham, J. Lumin. **8**, 344 (1974).
[2] J.L. Sommerdijk, A. Bril, and A.W. de Jager, J. Lumin. **8**, 341 (1974).
[3] E. Bayer, W. Rossner, B.C. Grabmaier, R. Alcalda, and G. Blasse, Chem. Phys. Lett. **216**, 228 (1993).
[4] E. van der Kolk, P. Dorenbos, C.W.E. van Eijk, A.P. Vink, C. Fouassier, and F. Guillen, J. Lumin. **97**, 212 (2002).
[5] E. van der Kolk, P. Dorenbos, and C.W.E. van Eijk, Opt. Commun. **197**, 317 (2001).
[6] A.M. Srivastava and W.W. Beers, J. Lumin. **71**, 285 (1997).
[7] E. van der Kolk, P. Dorenbos, and C.W.E. van Eijk, J. Phys.: Condens. Matter **13**, 5471 (2001).
[8] A.M. Srivastava and D.A. Doughty, J. Electrochem. Soc. **143**, 4113 (1996).
[9] A.M. Srivastava and D.A. Doughty, J. Electrochem. Soc. **144**, L190 (1997).
[10] E. Bayer, J. Leppert, B.C. Grabmaier, and G. Blasse, Appl. Phys. A: Mater. Sci. Process. **A61**, 177 (1995).
[11] E. van der Kolk, P. Dorenbos, A.P. Vink, R.C. Perego, C.W.E. van Eijk, and A.R. Lakshmanan, Phys. Rev. B **64**, 195129 (2001).
[12] A.P. Vink, E. van der Kolk, P. Dorenbos, and C.W.E. van Eijk, J. Alloys Comps. **341**, 338 (2002).
[13] P. Kisliuk and C.A. Moore, Phys. Rev. **160**, 307 (1967).
[14] J.M.P.J. Verstegen and J.L. Sommerdijk, J. Lumin. **9**, 297 (1974).
[15] R.A. Hewes and M.V. Hoffman, J. Lumin. **3**, 261 (1971).
[16] R. Alcala, D.K. Sardar, and W.A. Sibley, J. Lumin. **27**, 273 (1982).
[17] A. Meijerink, J. Lumin. **55**, 125 (1993).
[18] Y. Shen and K.L. Bray, Phys. Rev. B **58**, 11 944 (1998).
[19] A. Meijerink, J. Nuyten, and G. Blasse, J. Lumin. **44**, 19 (1989).
[20] J. Sytsma and G. Blasse, J. Lumin. **51**, 283 (1992).
[21] N. Yamashita, I. Yamamota, K. Ninagawa, T. Wada, Y. Yamashita, and Y. Nakao, Jpn. J. Appl. Phys., Part 1 **24**, 1174 (1985).
[22] G. Zimmerer, Nucl. Instrum. Methods Phys. Res. A **308**, 178 (1991).
[23] I. Sokolská, S. Kück, and M. Bakula, *SPIE Proceedings*

ICSSCL'2000 Zakopane (to be published 2002).
[24] A.P. Vink, P. Dorenbos, and C.W.E. van Eijk (unpublished).
[25] J.K. Lawson and S.A. Payne, Opt. Mater. **2**, 225 (1993).
[26] A.P. Vink, E.van der Kolk, P. Dorenbos, and C.W.E. van Eijk, Opt. Comm. (to be published 2002).
[27] C.G. Levey, T.J. Glynn, and W.M. Yen, J. Lumin. **31&32**, 245 (1984).
[28] S. Huang, X.-J. Wang, R.S. Meltzer, and W.M. Yen, J. Lumin. (to be published 2002).
[29] B.V. Andrievskii, V.Y. Kurlyak, N.A. Romanyuk, and Z.M. Ursul, Opt. Spectrosc. **66**, 364 (1989).
[30] K.H. Johnson and F.C. Smith, Jr., Chem. Phys. Lett. **7**, 541 (1970).